11. T. M. Brocher and M. J. Moses, *ibid. 93-276* (1993); T. M. Brocher and D. C. Pope, *ibid. 94-156* (1994).
12. R. M. Stewart and L. Peselnick, *J. Geophys. Res.* **82**, 2027 (1977).
13. J. M. Luetgert, *U.S. Geol. Surv. Open-File Rep. 88-238* (1988); C. Zelt and R. B. Smith, *Geophys. J. Int.* **108**, 16 (1992).
14. J. E. Ewing and M. Talwani, *J. Geophys. Res.* **96**, 6423 (1991); K. D. McIntosh, D. L. Reed, E. A. Silver, A. S. Meltzer, *ibid.*, p. 6459; A. S. Meltzer and A. R. Levander, *ibid.*, p. 6475; A. M. Trehu, *ibid.*, p. 6493; K. C. Miller, J. M. Howie, S. D. Ruppert, *ibid.* **97**, 19,961 (1992); J. M. Howie, K. C. Miller, W. U. Savage, *ibid.* **98**, 8173 (1993).
15. B. M. Page and T. M. Brocher, *Geology* **21**, 635 (1993).
16. T. M. Brocher, M. J. Moses, S. D. Lewis, *U.S. Geol. Surv. Prof. Pap.*, in press.
17. Reconnaissance refraction profiling in the San Francisco Bay Area was also interpreted in terms of a similar, simple two-layer crust by J. P. Eaton [*J. Geophys. Res.* **68**, 5789 (1963)], J. H. Healy [*J. Geophys. Res.* **68**, 5777 (1963)], and J. P. Eaton, *Calif. Div. Mines Geol. Bull.* **190**, 419 (1966). Constraints on the velocity and thickness of the lower crustal layer, however, were extremely limited from this earlier work, and no precritical reflections from it were obtained.
18. M. Liu and K. P. Furlong, *J. Geophys. Res.* **97**, 4941 (1992).
19. R. J. McLaughlin, W. P. Elder, K. McDougall, in *Geologic Excursions in Northern California: San Francisco to the Sierra Nevada*, D. Sloan and D. L. Wagner, Eds. (*Spec. Publ.* **109** California Divison of Mines and Geology, Sacramento, 1991), pp. 45–53.
20. R. C. Jachens, C. W. Roberts, A. Griscom, *Eos* (Fall Suppl.) **74**, 221 (1993).
21. A. W. Walter and W. D. Mooney, *Seismol. Soc. Am. Bull.* **72**, 1567 (1982); G. S. Fuis and W. D. Mooney, *U.S. Geol. Surv. Prof. Pap. 1515* (1990), p. 207.
22. R. H. Colburn and W. D. Mooney, *Seismol. Soc. Am. Bull.* **76**, 1305 (1986); W. S. Holbrook and W. D. Mooney, *Tectonophysics* **140**, 49 (1987).
23. K. P. Furlong and C. A. Langston, *Geophys. Res. Lett.* **17**, 1457 (1990).
24. P. A. Reasenberg and R. W. Simpson, *Science* **255**, 1687 (1992); K. P. Furlong and D. Verdonck, *U.S. Geol. Surv. Prof. Pap.*, in press; R. W. Simpson and P. A. Reasenberg, *ibid.*
25. I. G. Wong, R. W. Ely, A. C. Kollmann, *J. Geophys. Res.* **93**, 7813 (1988); J. P. Eaton, and M. J. Rymer, *U.S. Geol. Surv. Prof. Pap. 1487* (1990), p. 97.

26. We thank the National Earthquake Hazards Reduction and Offshore Geologic Framework Programs of the USGS (including USDI grants 14-34-92-G2213 to K.P.F., 14-34-93-G2309 to W.S.H. and 14-08-001-G2123 to T.V.M.), the National Science Foundation (including NSF grants EAR-91-04185 to K.P.F., EAR-91-17834 to S.L.K., and FD-91-17994 to T.V.M.), and CALTRANS for support. M. Iyer, A. Jayko, W. D. Mooney, and B. Page reviewed earlier drafts of this manuscript. The BASIX Working Group also includes: R. Anima, J. Childs, M. Marlow, T. Parsons, and U. ten Brink of the U.S. Geological Survey; R. Clymer, D. Jones, E. Karageorgi, J. Weber Band, and P. Williams of University of California Berkeley; and G. Thompson of Stanford University.

9 May 1994; accepted 11 July 1994

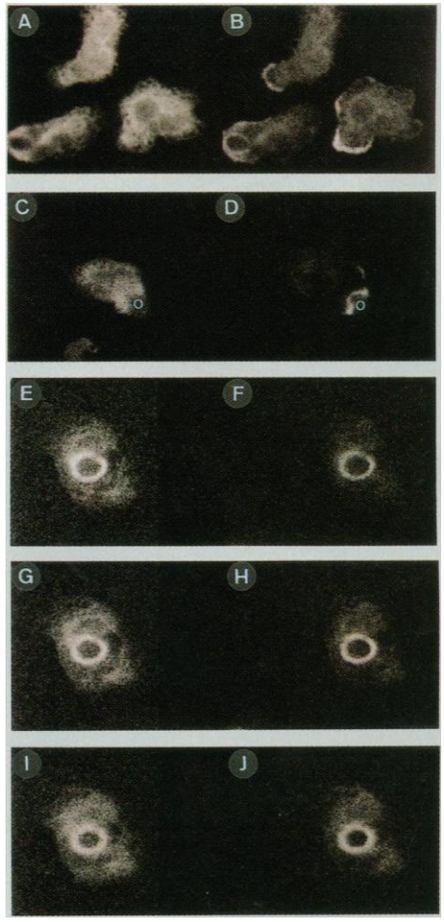

Fig. 1. Distribution of Ca^{2+}-ATPase (**A**, **C**, **E**, **G**, and **I**) and F-actin (**B**, **D**, **F**, **H**, and **J**) in resting and phagocytosing human neutrophils. Cells were purified as described (*4*) and allowed to adhere to glass slides and to phagocytose heat-killed yeast particles (*Saccharomyces cerevisiae*) that had been previously fixed to the slide (*20*). Each panel shows the rhodamine fluorescence (Ca^{2+}-ATPase) on the left and fluorescein fluorescence (F-actin) on the right. (A and B) Adherent nonphagocytosing neutrophils. (C and D) A neutrophil in the early stages of phagocytosis. Circles indicate the position of the yeast particle. (E through J) Three 1-μm-thick confocal serial sections through the top (E and F), center (G and H), and bottom (I and J) of the same neutrophil after completion of phagocytosis. The examples shown are typical of a total of 24 cells from a total of four experiments.

Redistribution of Intracellular Ca^{2+} Stores During Phagocytosis in Human Neutrophils

Olle Stendahl,* Karl-Heinz Krause, Joachim Krischer, Petra Jerström, Jean-Marc Theler, Robert A. Clark, Jean-Louis Carpentier, Daniel P. Lew

Subcellular gradients of cytosolic free Ca^{2+} concentration, $[Ca^{2+}]_i$, are thought to be critical for the localization of functional responses within a cell. A potential but previously unexplored mechanism for the generation of gradients of $[Ca^{2+}]_i$ is the accumulation of Ca^{2+} stores at the site of Ca^{2+} action. The distribution of the Ca^{2+} store markers Ca^{2+}-dependent adenosine triphosphatase and calreticulin was investigated in resting and phagocytosing human neutrophils. Both proteins showed an evenly distributed fine granular pattern in nonphagocytosing cells, but became markedly concentrated in the filamentous actin–rich cytoplasmic area around the ingested particle during phagocytosis. This redistribution began at early stages of phagocytosis and did not depend on an increase in $[Ca^{2+}]_i$. Thus, accumulation of Ca^{2+} stores in a restricted area of the cell may contribute to the generation of localized increases in $[Ca^{2+}]_i$.

The control of $[Ca^{2+}]_i$ is crucial for the regulation of cellular activity. In many cellular systems, focal, rather than generalized, changes in $[Ca^{2+}]_i$ occur, presumably serving to localize functional responses within the cell (*1*). Examples of Ca^{2+}-mediated localized responses include release of neurotransmitters from synaptic terminals (*2*), target cell lysis by cytotoxic T lymphocytes (*3*), and phagolysosome fusion in neutrophils (*4*). Localized changes in $[Ca^{2+}]_i$ can be generated by local increases in the concentration of the Ca^{2+}-releasing second messenger inositol triphosphate (IP_3) or by local activation of receptor-mediated Ca^{2+} influx. An alternative or additional mechanism, however, might be an accumulation of intracellular Ca^{2+} stores. In neutrophils, processing of phagocytosed microorganisms requires a focal activation of Ca^{2+}-dependent cellular functions (*5*). Because particle ingestion can be initiated at any part of the cell surface, localization of $[Ca^{2+}]_i$ increases by accumulation of Ca^{2+} stores would necessitate a rapid directed transport of these stores to the site of phagocytosis.

We tested the hypothesis that Ca^{2+} storage organelles accumulate at sites of Ca^{2+} action during phagocytosis in human neutrophils. Filamentous (F) actin distribution was monitored in parallel as a marker of the remodeling of the contractile machinery. Markers for Ca^{2+} stores include the Ca^{2+}-dependent adenosine triphosphatase (Ca^{2+}-ATPase) SERCA2b

O. Stendahl and P. Jerström, Department of Medical Microbiology, Linköping University, 58185 Linköping, Sweden.
K.-H. Krause and D. P. Lew, Division of Infectious Diseases, Hôpital Cantonal Universitaire, 1211 Geneva 14, Switzerland.
J. Krischer and J.-L. Carpentier, Department of Morphology, Centre Medical Universitaire, 1211 Geneva 4, Switzerland.
J.-M. Theler, Clinical Biochemistry, Centre Medical Universitaire, 1211 Geneva 4, Switzerland.
R. A. Clark, Department of Medicine, VA Medical Center and University of Iowa, Iowa City, IA 52242, USA.
*To whom correspondence should be addressed.

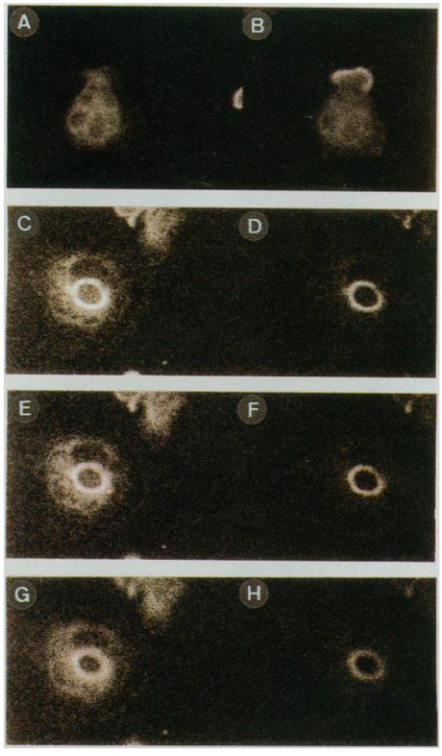

Fig. 2. Distribution of calreticulin (**A**, **C**, **E**, and **G**) and F-actin (**B**, **D**, **F**, and **H**) in resting and phagocytosing human neutrophils. Experimental procedures were as described (legend to Fig. 1), with the exception that a primary polyclonal rabbit antibody to recombinant human myeloid calreticulin (*11*) was used. Each panel shows the rhodamine fluorescence (calreticulin) on the left and fluorescein fluorescence (F-actin) on the right. (A and B) Adherent nonphagocytosing neutrophils. (C through H) Three 1-μm-thick confocal serial sections through the top (C and D), center (E and F), and bottom (G and H) of the same cell after completion of phagocytosis. The examples shown are typical of a total of 20 cells from a total of four experiments.

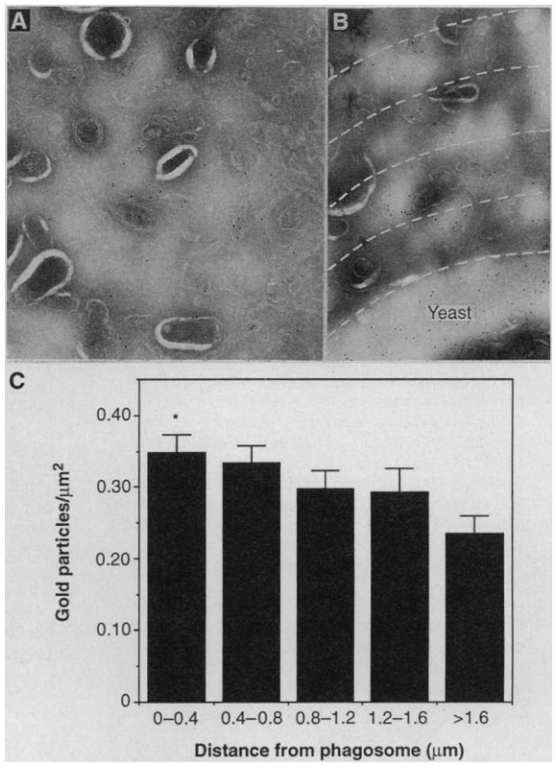

Fig. 3. Immunolocalization of calreticulin in the cytoplasm of human neutrophils. (**A**) Tubulovesicular structures labeled with the antibody to calreticulin. (**B**) Illustration of the quantification method; 0.4-μm-thick cytoplasmic bands were defined around the phagocytosed yeast particle. Phagocytosing neutrophils were prepared as described (*4*). For localization of calreticulin, the cells were centrifuged at 120*g* for 8 min and fixed in a mixture of 4% paraformaldehyde and 0.1% glutaraldehyde in ice-cold phosphate-buffered saline for 30 min at 22°C. The cells were then washed twice in phosphate-buffered saline and subjected to ultrathin cryosectioning. The sedimented cells were incubated for 1 hour in 2.3 M sucrose and cut as described (*21*). Thin sections were collected on nickel grids and immunolabeled with antibody to calreticulin and protein A–gold (10 nm) as described (*4*). Control incubations including protein A–gold alone and irrelevant antibodies showed no labeling. (**C**) Density of colloidal gold particles per square micrometer of cytoplasm in 0.4-μm-thick bands in the periphery of the phagosome. Two separate experiments were performed, and 39 and 85 fields that showed phagosomes were randomly selected and photographed at an initial magnification of ×17,400. The numbers of gold particles per square micrometer of four successive cytoplasmic circles (0.4 μm thick) around the phagosome, as well as the density of gold particles outside this perimeter, were evaluated on positive prints at a final magnification of ×52,200 on a graphic tablet (type 4943; Tektronics, Beaverton, Oregon) connected with a microprocessor system (IBM PC80). *$P < 0.005$ versus >1.6 μm from phagosome (Student's *t* test).

(*6*), the Ca^{2+}-binding protein calreticulin (*7*), and the IP_3-sensitive Ca^{2+} release channel (*8*); the latter may also localize to the plasma membrane in certain cell types (*9*) and has therefore not been included in the present analysis. We prepared antibodies to the NH_2-terminal sequence of the human nonmuscle Ca^{2+}-ATPase SERCA2b (*10*) and to recombinant human myeloid calreticulin (*11*). In immunoblots of total lysates or of microsomal fractions of human neutrophils, these antibodies recognized only 100-kD (Ca^{2+}-ATPase) and 60-kD (calreticulin) proteins, respectively (*12*).

Immunofluorescent staining of adherent, nonphagocytosing neutrophils with the antibody to Ca^{2+}-ATPase showed a fine granular pattern evenly distributed throughout the cytoplasm (Fig. 1A). Staining with fluorescent phalloidin to visualize F-actin showed a diffuse cytoplasmic and lamellopodia-associated distribution within the cell (Fig. 1B). We did not detect Ca^{2+}-ATPase in the actin-rich lamellopodia (Fig. 1A). During early stages of phagocytosis of yeast particles, F-actin localized predominantly to the advancing pseudopodia (Fig. 1D) (*5*). Concomitantly, the Ca^{2+}-ATPase content increased in the cytoplasmic area adjacent to the forming phagosome (Fig. 1C). After complete ingestion of the particles, both F-actin and Ca^{2+}-ATPase showed ringlike enrichment around the phagosome, observed in confocal serial sections from the top, center, and bottom of the adherent cell (Fig. 1, E through J).

Similar to the pattern observed with Ca^{2+}-ATPase, the homogeneous distribution of calreticulin observed in nonphagocytosing cells (Fig. 2A) changed to a ringlike localization around the phagosome after ingestion of yeast particles (Fig. 2, C, E, and G). The enrichment of periphagosomal fluorescence relative to cytosol was 2.7 ± 0.5 and 2.9 ± 0.9 (means ± SEM; $n = 10$) for Ca^{2+}-ATPase and calreticulin, respectively.

Thus, the distribution of Ca^{2+} storage organelles changed from relatively homogeneous in adherent nonphagocytosing cells to highly focal in phagocytosing cells. Because the accumulation of Ca^{2+} stores was observed around developing as well as completed phagosomes, it appears to be a relatively early event in phagocytosis and parallels the pattern of actin polymerization. Thus, it is possible that the actin cytoskeleton participates in the mechanism of Ca^{2+} store translocation; for example, through the association between the IP_3 receptor and the cytoskeletal protein ankyrin (*13*). However, accumulation of Ca^{2+} stores does not occur during formation of lamellopodia, demonstrating that it is not simply a function of actin polymerization.

We investigated the accumulation of Ca^{2+} stores at high resolution. As determined by electron microscopy on ultracryomicrotomy sections, calreticulin was associated with membrane-limited structures (Fig. 3A). The labeling density was highest in close proximity to the phagosome and decreased progressively as a function of distance from the phagocytosed particle (Fig. 3, B and C).

Given that $[Ca^{2+}]_i$ may be an important signal for the intracellular translocation of organelles (*14*), localized increases in $[Ca^{2+}]_i$

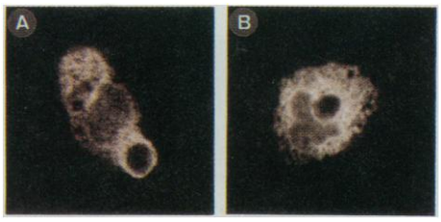

Fig. 4. Distribution of Ca^{2+}-ATPase (**A**) and lactoferrin (**B**) during phagocytosis in Ca^{2+}-depleted human neutrophils. Immunofluorescence was performed as described (legend to Fig. 1). Because both antibodies were from rabbits, experiments were performed in different cells. Neutrophils were depleted of Ca^{2+} by incubation for 1 hour at 37°C with 25 mM MAPT-AM in Ca^{2+}-free Krebs-Ringer solution supplemented with 1 mM EGTA. The examples shown are typical of a total of 10 cells from a total of two experiments.

around the phagosome might be the cause, rather than the consequence, of the accumulation of Ca^{2+} storage organelles. To test this hypothesis, we studied the distribution of Ca^{2+}-ATPase during phagocytosis in Ca^{2+}-depleted neutrophils ($[Ca^{2+}]_i < 20$ nM) that had been incubated with 1,2-bis-5-methylamino-phenoxylethane-*N*,*N*,*N*′,*N*′-tetraacetoxymethyl acetate (MAPT-AM). Particle ingestion is not impaired under these conditions, whereas the subsequent Ca^{2+}-sensitive translocation of secretory granules to the phagosome is completely blocked (*4*, *15*). In Ca^{2+}-depleted cells, the granule marker lactoferrin no longer accumulated around the ingested particle (Fig. 4B). However, Ca^{2+}-ATPase preferentially localized to the periphagosomal area in both Ca^{2+}-depleted (Fig. 4A) and normal neutrophils (Fig. 1E). Thus, an increase in $[Ca^{2+}]_i$ is not a necessary signal for the accumulation of Ca^{2+} stores during phagocytosis.

The physiological role of Ca^{2+} store accumulation during phagocytosis may be to generate subcellular $[Ca^{2+}]_i$ gradients. To investigate whether this occurs under our experimental conditions, we used double-excitation on-line $[Ca^{2+}]_i$ imaging (*16*) to analyze $[Ca^{2+}]_i$ during phagocytosis of yeast particles by neutrophils. During the first 10 s after particle attachment, the increase in $[Ca^{2+}]_i$ appeared to be homogeneous throughout the entire cell. In contrast, at later time points of phagocytosis, 11 of 13 analyzed cells showed a gradient of $[Ca^{2+}]_i$; 1 min after particle attachment, the $[Ca^{2+}]_i$ in the periphagosomal space was 90.2 ± 9.7 nM greater than the basal concentration, as opposed to 53 ± 10 nM greater than the basal concentration in the tail region (mean ± SEM, $n = 11$; $P < 0.001$, paired *t* test). These results confirm that during phagocytosis in neutrophils, the increases in $[Ca^{2+}]_i$ are greater in the periphagosomal space (*17*).

Our results demonstrate that Ca^{2+} storage organelles undergo spatial reorganization during cellular activation. Ca^{2+} stores may localize to specific areas of the cell, such as the synaptic terminals of the vertebrate retina (*18*). It has also been suggested that Ca^{2+} stores in neurons are transported from the site of synthesis at the rough endoplasmic reticulum to strategic loci, such as spines of synaptic connections (*19*). Our results show that in neutrophils the transport of Ca^{2+} stores to sites of Ca^{2+} action is a rapid, precisely controlled event that occurs during cellular activation.

The regulation of localized increases in $[Ca^{2+}]_i$ by accumulation of Ca^{2+} stores at the site of Ca^{2+} action has theoretical advantages over a mechanism that relies exclusively on the localized generation of IP_3. Thus (i) the total amount and the rate of IP_3-induced Ca^{2+} release would be expected to increase in proportion to the extent of accumulation of Ca^{2+} stores; (ii) the Ca^{2+} reuptake and storage capacity would also be expected to increase, thereby allowing a more precisely controlled termination of the $[Ca^{2+}]_i$ response; and (iii) the triggering of signaling steps distal to an increase in $[Ca^{2+}]_i$ would be minimized in functionally unimportant subcellular domains. The cell would therefore be able to regulate its Ca^{2+} response through a relatively low number of Ca^{2+} storage organelles concentrated at the site of Ca^{2+} action, rather than through an excess of uniformly distributed Ca^{2+} stores.

REFERENCES AND NOTES

1. P. W. Marks and F. R. Maxfield, *Cell Calcium* **11**, 181 (1990); R. A. Brundage, K. E. Fogarty, R. A. Tuft, F. S. Fay, *Science* **254**, 703 (1991); D. A. Williams, K. E. Fogarty, R. Y. Tsien, F. S. Fay, *Nature* **318**, 558 (1985); M. P. Mattson, M. Murain, P. B. Guthrie, *Dev. Brain Res.* **52**, 201 (1990); R. V. Yelamarty *et al.*, *J. Clin. Invest.* **85**, 1799 (1990).
2. S. J. Smith and G. J. Augustine, *Trends Neurosci.* **11**, 458 (1988).
3. M. Poenie, R. Y. Tsien, A. M. Schmitt-Verhulst, *EMBO J.* **6**, 2223 (1987).
4. M. E. E. Jaconi *et al.*, *J. Cell Biol.* **110**, 1555 (1990).
5. N. H. Valerius, O. Stendahl, J. H. Hartwig, T. Stossel, *Cell* **24**, 195 (1981).
6. J. Lytton and D. H. MacLennan, *J. Biol. Chem.* **263**, 15024 (1988); A. M. Gunteski-Hamblin, J. Greeb, G. E. Shull, *ibid.*, p. 15032; S. E. Burk, J. Lytton, D. H. MacLennan, G. E. Shull, *ibid.* **264**, 18561 (1989); A. K. Grover and I. Khan, *Cell Calcium* **13**, 9 (1992).
7. M. Michalak, R. E. Milner, K. Burns, M. Opas, *Biochem. J.* **285**, 681 (1992); K. H. Krause, *FEBS Lett.* **285**, 225 (1991); ———, K. B. Simmerman, L. R. Jones, K. P. Campbell, *Biochem. J.* **270**, 545 (1990); C. Van Delden *et al.*, *ibid.* **281**, 651 (1992).
8. C. A. Ross *et al.*, *Nature* **339**, 468 (1989); T. Furuichi *et al.*, *ibid.* **342**, 32 (1989); G. A. Mignery, T. C. Südhof, K. Takei, P. Camilli, *ibid.*, p. 192; D. L. Gill, *ibid.*, p. 16.
9. T. Fujimoto, N. Shinji, A. Miyawaki, K. Mikoshiba, K. Ogawa, *J. Cell Biol.* **119**, 1507 (1992); A. A. Khan, J. P. Steiner, S. H. Snyder, *Proc. Natl. Acad. Sci. U.S.A.* **89**, 2849 (1992).
10. S. Arber, K. H. Krause, P. Caroni, *J. Cell Biol.* **116**, 113 (1992).
11. A full-length calreticulin complementary DNA (cDNA) was cloned from a myeloid HL-60 cell cDNA library and then subcloned into baculovirus with the pVL1393 transfer vector. The recombinant protein was expressed in Sf9 insect cells, purified to homogeneity by ion-exchange and molecular seive chromatography, mixed with Freund's adjuvant, and injected subcutaneously into a rabbit.
12. K. H. Krause, unpublished data; R. A. Clark, unpublished data.
13. L. Y. W. Bourguignon, H. Jin, N. Iida, N. R. Brandt, S. H. Zhang, *J. Biol. Chem.* **268**, 7290 (1993); S. K. Joseph and S. Samanta, *ibid.*, p. 6477.
14. E. Neher, *J. Physiol. (London)* **395**, 193 (1988); D. P. Lew *et al.*, *J. Cell Biol.* **102**, 2197 (1986); S. M. Ali, M. J. Geisow, R. D. Burgoyne, *Nature* **340**, 131 (1989).
15. F. Di Virgilio, D. P. Lew, T. Pozzan, *Nature* **310**, 691 (1984); D. P. Lew *et al.*, *ibid.* **315**, 509 (1985).
16. Neutrophils incubated with the fluorescent Ca^{2+} indicator fura-2 were allowed to adhere to glass cover slips and to phagocytose opsonized heat-killed yeast as described (*4*). Fluorescence emission (505 nm) from phagocytosing neutrophils was recorded with an intensified charge-coupled device camera at two excitation wavelengths (340 and 380 nm). The excitation wavelength was alternated at video rate in synchrony with the acquisition. Images were digitized, recursively filtered, divided, and displayed after calibration of the ratio image into a numerical scale of $[Ca^{2+}]_i$ with the image processor IMAGINE (Synoptics, Cambridge, UK). The $[Ca^{2+}]_i$ images were then stored on videotape for subsequent analysis. The system has been described in more detail [J. M. Thelen, C. B. Wollheim, W. Schlegel, *J. Recept. Res.* **11**, 627 (1991)]. To quantify the $[Ca^{2+}]_i$ gradient during phagocytosis, we analyzed $[Ca^{2+}]_i$ in two square windows (4 μm), one placed adjacent to the phagosome and one adjacent to the tail of the neutrophil (that is, at maximal distance from the phagosome).
17. W. Sawyer, D. G. Sullivan, L. Mandell, *Science* **230**, 663 (1985); J. C. Schwab, D. A. Leong, G. L. Mandell, *J. Leukocyte Biol.* **51**, 437 (1992); T. Murata, J. A. Sullivan, D. W. Sawyer, G. L. Mandell, *Infect. Immun.* **55**, 1784 (1987); T. Bengtsson, M. E. E. Jaconi, J. M. Theler, D. P. Lew, O. Stendahl, *Eur. J. Cell Biol.* **62**, 49 (1993).
18. Y. W. Peng, A. H. Sharp, S. H. Snyder, K. W. Yau, *Neuron* **6**, 525 (1991); H. Kasai, Y. X. Li, Y. Miyashita, *Cell* **74**, 669 (1993).
19. M. F. Rossier, J. W. Putney Jr., *Trends Neurosci.* **14**, 310 (1991).
20. After incubation for 5 to 10 min, the cells were fixed in 4% formaldehyde in phosphate-buffered saline for 60 min at 4°C. After washing in phosphate-buffered saline, the cells were permeabilized with 1% Triton X-100 and then incubated overnight with normal porcine immunoglobulin G. Incubation with primary and secondary antibodies was performed as described (*4*). The primary antibody was a rabbit antibody prepared against the NH_2-terminal sequence of human nonmuscle Ca^{2+}-ATPase (SERCA2b) (*10*). The secondary antibody was a rhodamine-coupled porcine antibody to rabbit immunoglobulin G (Dacopatts, Copenhagen, Denmark). Double staining with F-actin was performed with fluorescein-coupled phalloidin [T. Bengtsson, I. Rundquist, O. Stendahl, M. P. Wymann, T. Andersson, *J. Biol. Chem.* **263**, 17385 (1988)]. Rhodamine and fluorescein fluorescence was analyzed in parallel in the same cell with a confocal scanning laser microscope (Molecular Dynamics). The 488-nm line of the Ar laser was used at 10 mW and 30% maximum intensity in combination with an LP-500 dichroic beam splitter for fluorescence activation. For parallel detection of rhodamine and fluorescein fluorescence, dual detectors with 570 EFLP and 530 DF 30 barrier filters were used. The aperture was 100 μm in diameter. The microscope (Nikon Optophot, Tokyo, Japan) was equipped with a ×100, high numeric aperture (1.4) objective.
21. K. T. Tokuyasu, *Histochem. J.* **12**, 381 (1980).

22. We thank M. E. E. Jaconi, S. Iyer, E. Huggler, D. Pearson, K. Leidal, and K. Holmgren for help and advice and I. Olsson (Lund University, Lund, Sweden) for providing antiserum to human lactoferrin. Supported by grants from the Swiss National Science Foundation (32-30161.90, 32-32376.91, and 31-34093.92), Swedish Medical Research Council (5968), King Gustav V 80 Year Foundation, Swedish Association Against Rheumatism, and U.S. Department of Veterans Affairs.

14 October 1993; accepted 8 July 1994